JACS
JOURNAL OF THE AMERICAN CHEMICAL SOCIETY
Article
pubs.acs.org/JACS

$Rb_2CdBr_2I_2$: A New IR Nonlinear Optical Material with a Large Laser Damage Threshold

Qi Wu,[†] Xianggao Meng,[‡] Cheng Zhong,[†] Xingguo Chen,[†] and Jingui Qin*[,†]

[†]Department of Chemistry, Wuhan University, Wuhan, Hubei 430072, China
[‡]College of Chemistry, Central China Normal University, Wuhan, Hubei 430079, China

Supporting Information

ABSTRACT: This paper describes the synthesis, crystal structure, and photophysical properties of a new compound $Rb_2CdBr_2I_2$. It crystallizes in the noncentrosymmetric space group *Ama*2. In the crystal, all the distorted tetrahedron $[CdBr_2I_2]^{2-}$ groups are arranged in a way such that all the Cd−I bonds are located in the same side of the Cd atoms resulting in a net polarization. $Rb_2CdBr_2I_2$ showed a powder second harmonic generation (SHG) response 4 times that of KH_2PO_4 (KDP). The preliminary measurement indicated that it exhibits a large laser-induced damage threshold (LDT) of 190 MW/cm^2 which is 6 times that of $AgGaS_2$. It also exhibits a wide transparent region (0.37−14 μm) with a relatively high (up to 490 °C) thermal stability. All these indicate that $Rb_2CdBr_2I_2$ is a new promising candidate for NLO materials in the IR region.

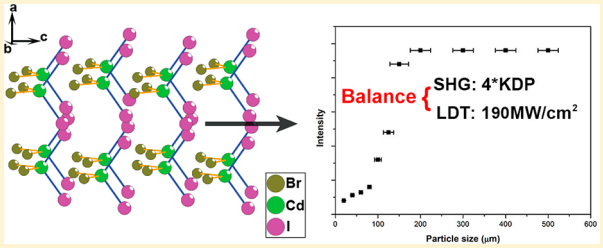

INTRODUCTION

Nonlinear optical (NLO) materials are of current interest and great importance because of their applications in photonic technologies.[1,2] Several crystals have been widely used in ultraviolet (UV) and visible regions in the past, such as KH_2PO_4 (KDP),[3] $KTiOPO_4$ (KTP),[4] $LiNbO_3$,[5] β-BaB_2O_4 (BBO),[6] LiB_3O_5 (LBO),[7] and $KBe_2BO_3F_2$ (KBBF).[8] On the other hand, the commercial NLO crystals in the (IR) region such as $AgGaS_2$,[9] $AgGaSe_2$,[10] and $ZnGeP_2$[11] have some drawbacks including the difficulty to grow high-quality crystals and low laser damage threshold (LDT).[12] In particular, the latter influenced their applications more heavily. Therefore, search for new IR NLO crystals with a high LDT is still a challenging subject in this field.

It has been accepted that thermal and electronic effects caused by strong optical absorption of the materials will lead to laser damage, and small band gaps of the current semiconductive IR NLO crystals are the main intrinsic reason for the laser damage.[13,14] On the other hand, it has been also accepted that the materials with large band gaps always show small NLO coefficients.[15] Therefore, it is necessary to undertake careful molecular engineering to design a new compound which can balance the conflicting factors mentioned above in order to discover the new IR NLO crystals with excellent comprehensive performance. Recently, we have found that partially replacing I^- with Cl^- in $Cs_2Hg_3I_8$[16] leads to a new compound, $Cs_2HgCl_2I_2$,[17] whose band gap was increased from 2.56 to 3.15 eV, and the LDT was increased to 83 MW/cm^2; however, the NLO effect was much weaker than in $Cs_2Hg_3I_8$. Therefore, search for new materials with high LDT and moderate SHG response simultaneously is a very important task in this field.

Our group has previously reported a known compound, $RbCdI_3{\cdot}H_2O$;[18] its SHG effect is 3.6 times that of KDP. But the infrared absorption and the low thermal stability limited its application in the IR region owing to the existence of the crystalline water in the structure. In the present work, on the basis of our experience described in the previous paragraph, we would like to try to partially replace I^- with Br^- (but not Cl^-) so as to achieve the balance of NLO and LDT. As a result, we have recently designed a first rubidium cadmium mixed halide, $Rb_2CdBr_2I_2$. To the best of our knowledge, no cadmium mixed halide NLO material has been reported so far. $Rb_2CdBr_2I_2$ exhibits a moderate powder second harmonic generation (SHG) property 4 times that of KH_2PO_4 (KDP). In comparison with many commercial IR NLO crystals, it exhibits a much higher laser-induced damage threshold (about 190 MW/cm^2). It also shows a wide transmission window in the IR range (up to 14 μm) and relatively high thermal stability (up to 490 °C). Its single crystal can be easily grown by slow evaporation of solvent in aqueous solution. Herein, it is believed that $Rb_2CdBr_2I_2$ is a new candidate for NLO materials in the IR region.

EXPERIMENTAL SECTION

Reagents. All starting materials were commercially available from Sinopharm, of analytical grade, and used without further treatment.

Synthesis of $Rb_2CdBr_2I_2$. RbBr (0.3308 g, 2 mmol), CdI_2 (0.3662 g, 1 mmol), and 5 mL of deionized water were loaded into a 23 mL Teflon-lined autoclave and subsequently sealed. The autoclave was heated to 230 °C for 1 day and then cooled slowly to room

Received: December 5, 2013
Published: March 31, 2014

dx.doi.org/10.1021/ja412405u | J. Am. Chem. Soc. 2014, 136, 5683−5686

temperature. After filtration, the filtrate was slowly volatilized at 40 °C. A few days later, some colorless block crystals (0.6700 g, 0.96 mmol) were harvested with the different size up to 4 × 2 × 1 mm^3 and the yield of 96% (based on the mass of CdI_2 or RbBr), and were washed with deionized water (a photograph of the crystal is shown in Figure S1 in the Supporting Information).

Single Crystal Structure Determination. Single crystal X-ray diffraction data were collected at 298 (K) using a Bruker SMART APEX diffractometer equipped with a CCD detector (graphite-monochromated Mo Kα radiation, λ = 0.71073 Å). A transparent block of crystal of $Rb_2CdBr_2I_2$ with dimensions of ca. 0.10 × 0.10 × 0.10 mm^3 was mounted on a glass fiber with epoxy for structure determination. The software package SAINT PLUS[19] was used for date set reduction and integration for $Rb_2CdBr_2I_2$. The structure of $Rb_2CdBr_2I_2$ is solved by direct methods and refined using the SHELXTL 97 software package.[20] Relevant crystallographic data are summarized in Table 1; selected bonds and angles are listed in Table 2. The CCDC number is 989832.

Table 1. Crystallographic Data for $Rb_2CdBr_2I_2$

formula	$Rb_2CdBr_2I_2$
fw	696.96
T/K	298(2)
wavelength/Å	0.710 73
crystal color	colorless
space group	*Ama*2
a/Å	11.764(8)
b/Å	12.025(8)
c/Å	8.446(6)
α/deg	90
β/deg	90
γ/deg	90
volume/$Å^3$	1194.8(14)
Z	4
dcalcd/g cm^{-3}	3.874
F(000)	1192
reflections collected	3935
independent reflections	1118 [R(int) = 0.0515]
R1, wR2 [$I > 2\sigma(I)$]	0.0557/0.1760
R1, wR2 (all data)	0.0614/0.1819
min/max $\Delta\rho$/e$Å^{-3}$	−1.700/2.114

Table 2. Bond lengths (Å) and Angles (deg) for $Rb_2CdBr_2I_2$

Br(1)−Cd(1)	2.599(4)
Cd(1)−Br(2)	2.659(4)
Cd(1)−I(1)#2	2.750(2)
Cd(1)−I(1)	2.750(2)
Br(1)−Cd(1)−Br(2)	107.40(15)
Br(1)−Cd(1)−I(1)#2	108.51(7)
Br(2)−Cd(1)−I(1)#2	111.43(8)
Br(1)−Cd(1)−I(1)	108.51(7)
Br(2)−Cd(1)−I(1)	111.43(8)
I(1)#2-Cd(1)−I(1)	109.45(11)

Powder X-ray Diffraction. X-ray diffraction patterns of polycrystalline material were obtained at room temperature on Bruker D8 Advanced diffractiometer with Cu Kα_1 radiation (λ = 1.54186 Å) in the range of 10−70° at a scanning rate of 0.5°/min. The powder XRD patterns for the pure powder samples of $Rb_2CdBr_2I_2$ showed good agreement with the calculated XRD patterns from the single-crystal models (see Figure S2 in the Supporting Information).

Infrared Spectrum and UV−Vis Diffuse Reflectance Spectrum. The IR spectrum was recorded on a NICOLET 5700 Fourier-transformed infrared (FTIR) spectrophotometer in the 4000−700 cm^{-1} region (2.5−14 μm) using the attenuated total reflection (ATR) technique with a germanium crystal. The UV−vis diffuse reflectance spectrum was recorded on a Varian Cary 5000 UV−vis−NIR spectrophotometer in the region 200−800 nm. A $BaSO_4$ plate was used as the standard (100% reflectance), on which the finely ground samples from the crystals were coated. The absorption spectrum was calculated from reflectance spectrum using the Kubelka−Munk function:[21] $\alpha/S = (1 - R)^2/2R$, where α is the absorption coefficient, S is the scattering coefficient, and R is the reflectance.

NLO Property and LDT Measurement. Powder second-harmonic generation (SHG) signals were measured using the method adapted from Kurtz and Perry.[22] A pulsed Q-switched Nd:YAG laser was utilized to generate fundamental 1064 nm light with a pulse width of 10 ns. The samples were pressed between two glasses. To make relevant comparisons with known SHG materials, microcrystalline KH_2PO_4 (KDP) served as the standard. Both the powders of $Rb_2CdBr_2I_2$ and KDP were ground and sieved into the same particle size (100−140 μm). Since phase-matchable SHG materials are very important owing to their applications, we search for the relationships between SHG efficiencies and particle sizes. Polycrystalline samples were ground and sieved into the following particle size ranges: 20−40, 40−60, 60−80, 80−100, 100−125, 125−150, 150−200, 200−300, 300−400, and 400−500 μm. Laser-induced damage threshold (LDT) test was performed on very small crystalline samples without any pretreatment, with 1 Hz focused laser pulses emitted by the other laser source (1064 nm, 5 ns). The beam diameter is 150 μm. The energy of each pulse was measured to be about 0.17 mJ. To obtain the energy intensity of laser damage, an optical concave lens was used to adjust the diameter of the laser beam. The samples endured gradually enhanced radiation until their appearance changed under a magnifier after the irradiation.

Thermogravimetric Analysis. The TG scans were performed on a Setaram SETSYS-16 simultaneous analyzer instrument. Crystal samples (5 mg) were enclosed in Al_2O_3 crucibles and heated from room temperature to 1000 °C at a rate of 10 K/min under flowing nitrogen gas.

RESULTS AND DISCUSSION

Crystal Structure. Single-crystal X-ray diffraction data for $Rb_2CdBr_2I_2$ are presented in Table 1. It crystallizes into a crystal system orthorhombic with a noncentrosymmetric space group of *Ama*2. Its cell parameters are a = 11.764(8) Å, b = 12.025(8) Å, c = 8.446(6) Å, $\alpha = \beta = \gamma = 90°$, Z = 4. Selected bond lengths and angles are listed in Table 2.

As shown in Figure 1a, there are two independent Cd^{2+} cations, and each of them forms $[CdBr_2I_2]^{2-}$ distorted tetrahedron anion group. Two Cd−Br bond lengths (2.659(4) and 2.599(4) Å) are shorter than two Cd−I bonds (2.750(2)Å). All the Cd−I bonds are located in the right-hand side of Cd atoms (see Figure 1b). This arrangement in the crystal structure results in a net polarization parallel to c axis (indicated by the large black arrow in Figure 1b). It is due to this net polarization that a substantial SHG response is observed.

Infrared Spectrum and UV−Vis Diffuse Reflectance Spectrum. The FTIR spectrum of the powder compound is shown in Figure 2. It exhibits wide transparent range from 4000 to 700 cm^{-1} (2.5−14 μm) without any absorption. The UV−vis diffuse reflectance spectrum for the compound is shown in Figure 3. The spectrum shows that the absorption edge near the UV side is at about 306 nm; therefore, its powder shows a wide transparence in the visible and IR region from 0.37 to 14 μm. The band gap of the compound can be calculated to be 3.35 eV, which is much higher than that of commercially available IR NLO crystals such as $AgGaS_2$, $AgGaSe_2$, and $ZnGeP_2$, implying that $Rb_2CdBr_2I_2$ may exhibit a higher laser-induced damage threshold (LDT).

dx.doi.org/10.1021/ja412405u | J. Am. Chem. Soc. 2014, 136, 5683−5686

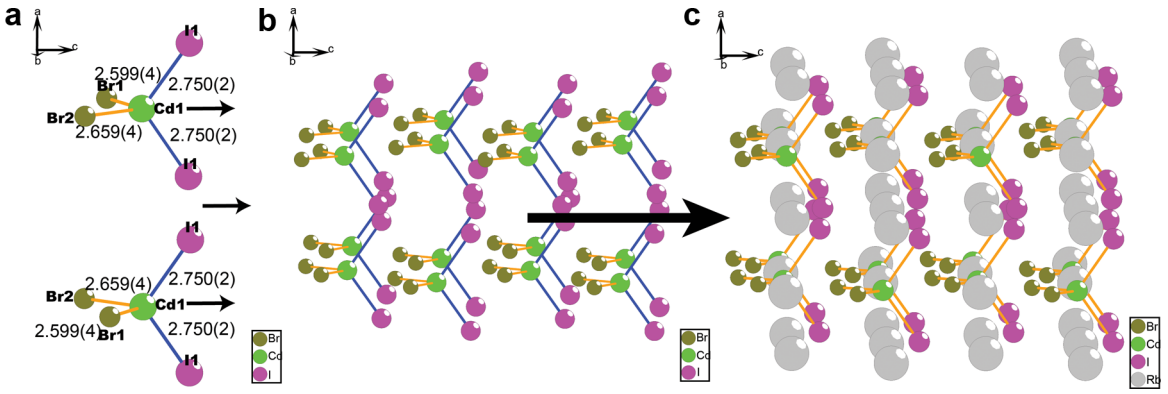

Figure 1. (a) $CdBr_2I_2$ tetrahedral groups (each Cd^{2+} is bonded to two iodine atoms and two bromine atoms). (b) Ball-and-stick diagrams of $Rb_2CdBr_2I_2$ (Rb atoms are omitted for clarity). All the Cd−I bonds are located in the same side of Cd atoms, leading to a net polarization parallel to *c* axis. (c) Ball-and-stick diagrams of $Rb_2CdBr_2I_2$.

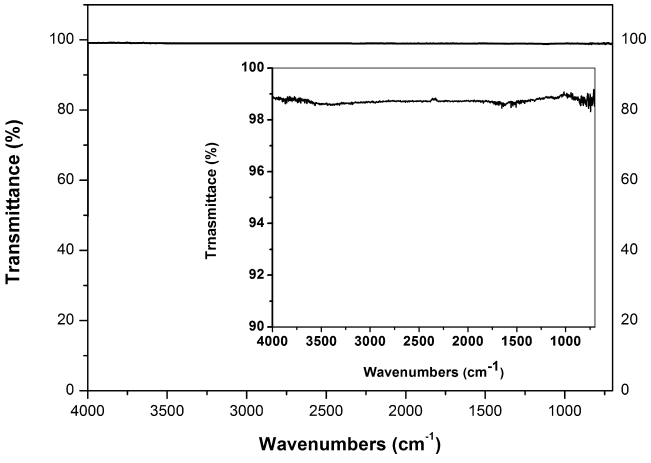

Figure 2. FTIR spectrum for $Rb_2CdBr_2I_2$(4000−700 cm^{-1} region).

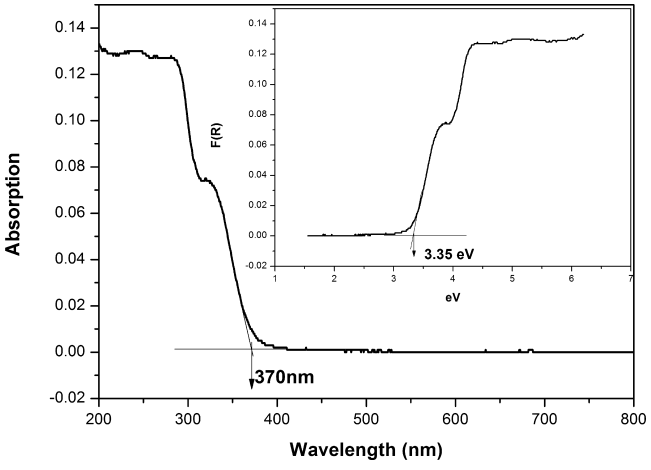

Figure 3. UV−vis absorption spectrum for $Rb_2CdBr_2I_2$.

Thermogravimetric Analysis. The thermal behavior of $Rb_2CdBr_2I_2$ is shown in Figure 4. The compound is thermally stable up to about 490 °C when it starts losing weight, and it continues to lose weight until about 900 °C to reach a platform. This indicates that its thermal stability is quite high among the halides containing iodide anion.

NLO Properties and LDT Measurements. We measured the SHG performance of the compound using a laser with a wavelength of 1064 nm and a pulse width of 10 ns. It showed

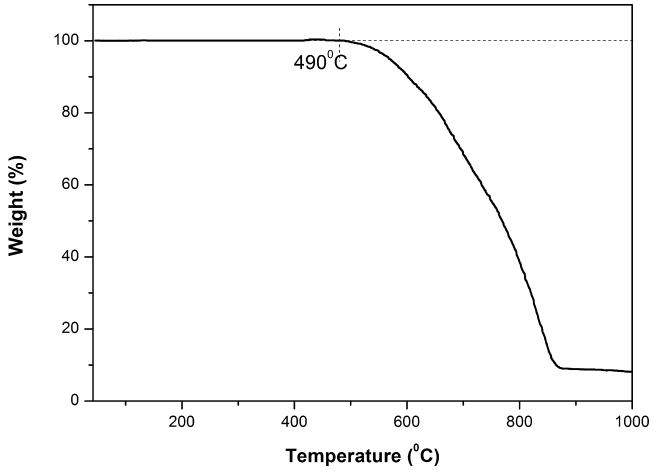

Figure 4. Thermogravimetric analysis curve for $Rb_2CdBr_2I_2$ crystal.

powder SHG efficiencies as strong as 4 times that of KDP. Study of the SHG intensity as a function of particle size is shown in Figure 5. The powder SHG intensity rises with the increase in the particle size from 20 to 500 μm, and then it reaches a plateau when the particle size increases further, which indicates that the SHG effect of the compound is type 1 phase-

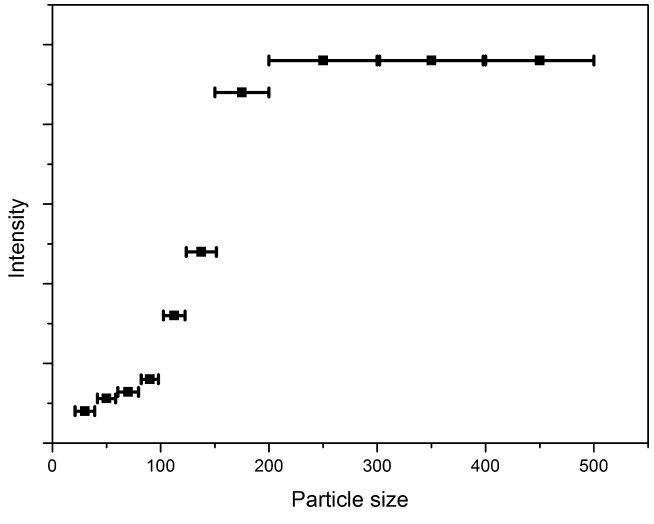

Figure 5. Phase-matching curve for $Rb_2CdBr_2I_2$.

dx.doi.org/10.1021/ja412405u | J. Am. Chem. Soc. 2014, 136, 5683−5686

matchable. A preliminary examination of the laser-induced damage threshold has been carried out on small crystalline samples with a Q-switched laser source. The samples showed a damage threshold of about 190 MW/cm^2 (1064 nm, 5 ns). This value is much higher than that of $AgGaS_2$ (AGS), and the latter is a commercially used IR NLO crystal with the LDT at about 30 MW/cm^2.[23]

CONCLUSION

In summary, a rubidium cadmium mixed halide $Rb_2CdBr_2I_2$ has been created and synthesized for the first time. A single crystal of size 4 × 2 × 1 mm^3 has been grown by slow solvent evaporation in aqueous solution. Its powders showed a moderate type 1 phase-matchable SHG response 4 times that of KDP. More importantly, it showed high laser damage threshold (190 MW/cm^2) which is 6 times that of $AgGaS_2$. Its powder also showed a wide transparence in the visible and IR region (0.37−14 μm) with a relatively high thermal stability. All these properties make the compound a potential IR NLO material. The results have given some useful information to support an approach for achieving the better balance between SHG and LDT through the rational design strategy which introduces a suitable second halide anion to make a new mixed halide as new NLO materials.

ASSOCIATED CONTENT

Supporting Information

Photograph of the single crystal of $Rb_2CdBr_2I_2$, powder X-ray diffraction pattern data, EDX spectrum, the proportion of element in $Rb_2CdBr_2I_2$ by EDX, and crystal data (CIF). This material is available free of charge via the Internet at http://pubs.acs.org.

AUTHOR INFORMATION

Corresponding Author

jgqin@whu.edu.cn

Notes

The authors declare no competing financial interest.

ACKNOWLEDGMENTS

This work was financially supported by the National Basic Research Project of China (No. 2010CB630701) and the Natural Science Foundation of China (No. 91022036). The authors thank Dr. Xiaomao Li of the Technical Institute of Physics and Chemistry, Chinese Academy of Sciences, for measuring the Laser damage threshold of the sample.

REFERENCES

(1) Chen, C. T.; Liu, G. Z. *Annu. Rev. Mater. Sci.* **1986**, *16*, 203.
(2) (a) Halasyamani, P. S.; Poeppelmeier, K. R. *Chem. Mater.* **1998**, *10*, 2753. (b) Ok, K. M.; Halasyamani, P. S. *Chem. Soc. Rev.* **2006**, *35*, 710.
(3) Smith, W. L. *Appl. Opt.* **1977**, *16* (7), 798.
(4) Kato, K. *IEEE J. Quantum Electron.* **1991**, *27*, 1137.
(5) Boyd, G. D.; Miller, R. C.; Nassau, K.; Bond, W. L.; Savage, A. *Appl. Phys. Lett.* **1964**, *5* (11), 234.
(6) Chen, C.; Wu, B.; Jiang, A.; You, G. *Sci. Sin., Ser. B* **1985**, *28* (3), 235.
(7) Chen, C.; Wu, Y.; Jiang, A.; Wu, B.; You, G.; Li, R.; Lin, S. *J. Opt. Soc. Am. B* **1989**, *6* (4), 616.
(8) Chen, C. T.; Wang, Y.; Xia, Y. N.; Wu, B. C.; Tang, D. Y.; Wu, K. C.; Zeng, W. R.; Yu, L. H.; Mei, L. F. *J. Appl. Phys.* **1995**, *77*, 2268.
(9) Chemla, D. S.; Kupecek, P. J.; Robertson, D. S.; Smith, R. C. *Opt. Commun.* **1971**, *3*, 29.
(10) Boyd, G. D.; Kasper, H. M.; McFee, J. H.; Storz, F. G. *IEEE J. Quantum Electron.* **1972**, *8*, 900.
(11) Boyd, G. D.; Buehler, E.; Storz, F. G. *Appl. Phys. Lett.* **1971**, *18*, 301.
(12) Dmitriev, V. G.; Gurzadyan, G. G.; Nikogosyan, D. N. *Handbook of Nonlinear Optical Crystals*, 3rd ed.; Springer-Verlag: Berlin, 1999.
(13) Lin, X.; Zhang, G.; Ye, N. *Cryst. Growth Des.* **2009**, *9*, 1186.
(14) Yin, W.; Feng, K.; He, R.; Mei, D.; Lin, Z.; Yao, J.; Wu, Y. *Dalton Trans.* **2012**, *41*, 5653.
(15) Jackson, A. G.; Ohmer, M. C.; LeClair, S. R. *Infrared Phys. Technol.* **1997**, *38*, 233.
(16) Zhang, G.; Qin, J.; Liu, T.; Zhu, T.; Fu, P.; Wu, Y.; Chen, C. *Cryst. Growth Des.* **2008**, *8*, 2946.
(17) Zhang, G.; Li, Y.; Jiang, K.; Zeng, H.; Liu, T.; Chen, X.; Qin, J.; Lin, Z.; Fu, P.; Wu, Y.; Chen, C. *J. Am. Chem. Soc.* **2012**, *134*, 14818.
(18) Ren, P.; Qin, J.; Liu, T.; Wu, Y.; Chen, C. *Opt. Mater.* **2003**, *23*, 331.
(19) Sheldrick, G. M. *SHELXTL*, version 6.14; Bruker Analytical Xray Instruments, Inc.: Madison, WI, 2003.
(20) Sheldrick, G. M. *Acta Crystallogr.* **2008**, *A64*, 112.
(21) Wendlandt, W. M.; Hecht, H. G. *Reflectance Spectroscopy*; Interscience: New York, 1966; pp 62−65.
(22) Kurtz, S. K.; Perry, T. T. *J. Appl. Phys.* **1968**, *39*, 3798.
(23) Chandra, S.; Allik, T. H.; Catella, G.; Hutchinson, J. A. *Advanced Solid-State Lasers*; Bosenberg, W. R., Fejer, M. M., Eds.; OSA Trends in Optics and Photonics Series, Vol. *19*; OSA: Washington, DC, 1998; p 282.